ASSOCIATIE EURATOM-FOM

FOM-INSTITUUT VOOR PLASMAFYSICA

RIJNHUIZEN — NIEUWEGEIN — NEDERLAND

December 1985

ION TEMPERATURES IN TORTUR III

by

F.B. Hendriks and H.J.B.M. Brocken

Rijnhuizen Report 85-162

This work was performed as part of the research programme of the association agreement of Euratom
and the 'Stichting voor Fundamenteel Onderzoek der Materie' (FOM)
with financial support from the 'Nederlandse Organisatie voor Zuiver-Wetenschappelijk Onderzoek' (ZWO) and Euratom.

C O N T E N T S

ION TEMPERATURES IN TORTUR III

by

F.B. Hendriks
Association Euratom-FOM
FOM-Instituut voor Plasmafysica
Rijnhuizen, Nieuwegein, The Netherlands

and

H.J.B.M. Brocken
Max Planck Institut für Plasmaphysik,
Garching, W. Germany

ABSTRACT

Spatially resolved ion-energy distributions are presented for discharges in the TORTUR III tokamak.

The measurements are performed in an active method, using a neutral hydrogen probing beam of 20-30 keV, to enhance charge-exchange processes along its path, as well as by the usual passive method. Ion temperatures can amount up to 1 keV.

INTRODUCTION AND SUMMARY

The TORTUR III device is a small tokamak with major and minor radii of 0.46 and 0.09 m, respectively, designed to study current driven turbulent heating.

TORTUR I started to operate in 1975 to investigate the turbulent heating by extra current pulses due to large electric fields.

TORTUR II was a modified version: the quartz vacuum vessel was replaced by an inconel vessel to improve the wall conditions. Later a transformer yoke was installed enabling discharges up to 50 ms.

Since then the device, TORTUR III, is basically an ordinary tokamak with the provisions to study the current-driven turbulent heating in the plateau phase of a tokamak. Plateau currents up to 60 kA can be achieved during stable plasma confinement with a toroidal magnetic field up to 3.0 tesla.

Though the turbulent heating due to extra current pulses is an important subject to study in TORTUR, in this report ion temperature measurements as a function of time during quasi-stationary discharges without turbulent heating are presented.

However, even for these quasi-stationary discharges, from detailed measurements of the plasma state (loop voltages, plasma resistivity, impurity deduction, noise spectra) it is concluded that the plasma is in a current-driven weakly turbulent state: the plasma resistivity is a factor 2-4 times the classical resistivity, taking the impurity level ($Z_{eff} \approx 1.7 - 2.2$) properly into account.

Detailed analysis can be found in the references [13], [21], [22] and [23].

The reason for this anomalous quasi-turbulent state during the plateau is sought in the very fast current increase towards the plateau state, which is special for these TORTUR discharges ($dj/dt \geq 2\times10^7$ A/s).

The condition of high-current densities (drift parameter $v_d/c_s > 1$) is maintained after reaching the plateau.

As a consequence, broad spatial temperature and density profiles could be maintained with a plasma state characterized by relatively high values of beta-poloidal ($\beta_{pol} \lesssim 2$) and anomalous values of the resistivity.

The applied toroidal electric field (E ~ 3-10 V/m) is just sufficient to excite micro-instabilities. From noise spectra evidence exists that a quasi-stationary turbulent state is maintained with low frequency drift waves and higher frequency magnetic turbulence. Ion temperatures reached are always very near to the electron temperature, in some cases even higher, as will be shown in the examples.

The structure of this report is as follows: Chapter 1 deals with the derivation of the ion flux leaving the plasma during the presence of a probing beam and the factors which complicate the evaluation of the ion temperature.

In Chapter 2 the experimental arrangement and the analysing system is discussed.

In Chapter 3 results of measurements are shown.

Chapter 4 gives some conclusions about the results and the problems arising when using an injecting beam to obtain neutral particle energy spectra.

1. THEORETICAL BACKGROUND CONSIDERATIONS

1.1 A derivation of the ion flux with a probing beam

Even the so-called "fully ionized" high-temperature fusion plasmas are permeated by a low background density of neutral hydrogen atoms. As can be seen in Fig. 1, this is because, over most of the energy range of interest, the cross-section for charge exchange between hydrogen atoms and hydrogen ions ($\underline{H}^0 + H^+ \rightarrow \underline{H}^+ + H^0$) is much larger than the cross-section for electron impact ionization ($\underline{H}^0 + e^- \rightarrow \underline{H}^+ + 2e^-$) or for ion impact ionization ($\underline{H}^0 + H^+ \rightarrow \underline{H}^+ + H^+ + e^-$).

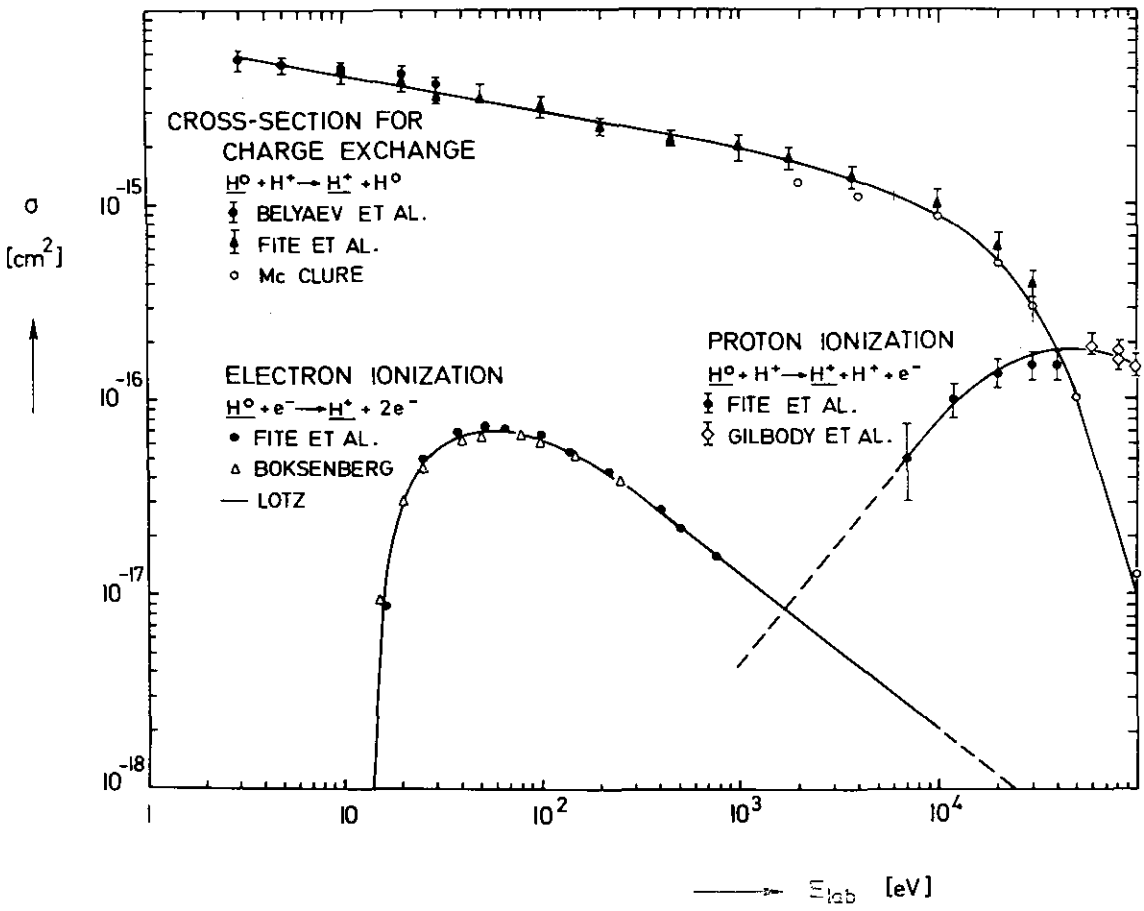

Fig. 1. Cross-sections for charge exchange, electron ionization and proton ionization of neutral hydrogen atoms in a hydrogen plasma. [1,16,17,18,19,20].

The determination of the ion temperature T_i can be performed from an analysis of the neutral particle flux if the plasma is transparent for charge-exchange atoms, i.e. when the optical thickness of the plasma, λ, with respect to these atoms satisfies the inequality $\lambda = n\sigma a < 1$, where n is the average plasma density, a the plasma radius and σ the total cross-section for neutrals changing into ions in the plasma. However, in devices where the plasma is semi-transparent or opaque for fast neutrals, as it is in TORTUR III, it is necessary to perform a detailed analysis of the processes by which the atoms can escape to the wall. In both cases the outgoing flux is an integral along the line-of-sight which complicates the local energy analysis strongly.

A much better method to determine the local plasma ion temperature is the use of a neutral particle beam to increase considerably the neutral background density along its trajectory above the ambient neutral background of the plasma. As a consequence the production of charge-exchange plasma ions is strongly enhanced locally. For the natural background of charge-exchange plasma ions, those present without the beam, can be corrected by subtraction.

An expression for the neutral particle flux, Γ_b, reaching the analyser in the presence of a probing beam, will be derived now.

Assuming a local maxwellian distribution of the plasma ions at radius r with temperature T(r) and plasma density n(r), the number density $\Delta n(r)$ of plasma ions with energies between E and $E+\Delta E$ is given by:

$$\Delta n(r) = \sqrt{4/\pi}\; n(r)\; \frac{E^{1/2}}{[k_B T(r)]^{3/2}}\; \exp\left[-\frac{E}{k_B T(r)}\right] \Delta E \; . \qquad (1)$$

The transmission of both the neutral beam into the plasma and of the charge-exchange neutral flux towards the analyser is given by:

$$A_{b,c}(r,E) = \exp\left[-\int_r^a \frac{s(x,E)}{v}\, dx\right] \; . \qquad (2)$$

A_b is the neutral beam transmission.

A_c denotes the charge-exchange neutral flux transmission.

$s(x,E) = [\langle\sigma_{ex} v\rangle_i + \langle\sigma^i_{ion} v\rangle_i + \langle\sigma^e_{ion} v\rangle_i] n(r)$ is the effective particle loss frequency due to charge exchange and impact ionization. The brackets denote averaging over the relevant maxwellian distributions of the colliding species.

An expression for the number of charge-exchange reactions per unit time and per energy interval at radius r is:

$$\Delta R(r,E) = n_b \Delta n(r) \langle \sigma_{ex} v \rangle_b \, A_b(r,E_b) dV \; . \qquad (3)$$

Here, n_b is the beam density, $\langle \sigma_{ex} v \rangle_b$ is the collision rate coefficient for charge exchange and dV is the considered volume element around a position r in the plasma.

On its way out of the plasma towards the analyser, the neutral flux is attenuated by a factor $A_c(r,E)$ (Eq. (2)), and the efficiency of the helium stripping cell due to re-ionization $\varepsilon_{eff}(E)$.

The flux of ions around r within the energy interval $[E, E + \Delta E]$ which enters the neutral energy analyser, is given by:

$$d\Gamma_b(r,E) = \frac{\Omega_p}{4\pi} \varepsilon_{eff}(E) \Delta R(r,E) A_c(r,E)$$

$$= \sqrt{4/\pi} \, \frac{\Omega_p}{4\pi} \, \varepsilon_{eff}(E) A_b(r,E_b) A_c(r,E) n_b n(r) \times$$

$$\times \langle \sigma_{ex} v \rangle_b \left[\frac{E}{k_B T(r)}\right]^{3/2} \exp\left[-\frac{E}{k_B T(r)}\right] \frac{\Delta E}{E} \, dV_{bp} . \qquad (4)$$

V_{bp} is the volume defined by the cross-section of the beam and the analyser-viewing field at r. V_{bp} is almost independent of r; the solid angle of the detector entrance slit as seen from the plasma is denoted by Ω_p. Though expression (4) ideally denotes the flux at radius r due to the presence of a probing beam of infinitely small cross-section, in reality the expression has to be averaged over the finite beam cross-section. All r-dependent quantities have to be profile-averaged. In our case the effective beam radius was 4 cm compared to a plasma cross-section of about 16 cm.

For the evaluation of the energy distribution the neutral particle flux, $d\Gamma_b(r,E)$ is first divided by the respective energy-dependent factors $\varepsilon_{eff}(E)$ and $A_c(r,E)$. Next, a semi-logarithmic plot $\ell n(d\Gamma_b/(\sqrt{E}\, dE))$ vs E is made. When the data permit the fitting of a significant straight line an ion temperature, averaged over the beam cross-section, can be deduced from the reciprocal slope.

1.2 Factors which complicate the evaluation of the local ion temperatures

In practice, several factors still complicate the evaluation of the local ion temperatures despite the use of a probing beam.

a. Variation of the beam energy does not change the charge-exchange flux very much in the range between 20 and 40 keV: increasing beam transmission due to a higher beam energy is compensated by a decrease of the cross-section for charge exchange. This gives the freedom to operate in a rather wide energy range of the probing beam. However, care has to be taken to avoid appreciable heating. For injection times larger than 2.5 ms at 25 kV, an increase of the ion temperature of 50 eV per ampere equivalent is calculated as an upper limit for TORTUR. Heating effects of the predicted magnitude have actually been observed.

b. The neutral density is strongly peaked near the plasma surface and so is the charge-exchange production rate of ionized beam particles. When de beam is present, the neutral density is increased by degassing due to collisions of the neutralized beam particles with the wall of the torus.

c. The measurements have to be corrected for the presence of charge-exchange neutrals emerging from the plasma itself. It is difficult to make a precise estimate of the magnitude of this contribution. Calculation of the production of neutrals arising from radiative recombination, performed by Dnestrovskij [2] and Brocken [3], show this effect to be small. Of course the experiment itself helps to judge this contribution of the background by turning off the probing beams.

d. Another effect perturbing the energy spectrum is the increase of the neutral background density due to charge exchange of plasma ions by the injected beam atoms. This effect will be estimated.
Let us assume that the neutral beam is ionized by charge exchange, which is the dominant process, for a considerable fraction of the beam density as it traverses the plasma. The resulting plasma neutrals emerge from the beam volume with thermal speed v_i until they become ionized. A statistical measure for the mean free path is $\lambda_i = v_i \tau_i$, where τ_i is the ionization time.

The neutralized atoms fill a cylindrical volume outside the original beam volume given by $(\pi a^2) \times (2\lambda_i)$, provided that the ion free path lies in the domain $a \leq \lambda_i < R$, where a and R are the minor and major radii respectively. Consequently, the neutral density is increased in this volume by an amount Δn_o given by:

$$\Delta n_o \approx \frac{I_b \tau_i}{2\pi a^2 e \lambda_\perp} = \frac{I_b}{2\pi a^2 e v_\perp} , \qquad (5)$$

where I_b is the transmitted neutral beam current in ampere equivalent ($I_b = \pi r_b^2 \, e v_b n_b$).
This spurious increase of the neutral density resulting from charge exchange of plasma ions gives rise to an additional induced flux $d\Gamma_o(E)$ of charge-exchange plasma ions in a region outside the primary beam volume (multiple charge-exchange effect).
Consequently, the energy spectrum is deformed in the lower energy range due to the radial temperature profile. This results in a lower limit for the validity of the energy range of the active beam-probing method. The lower limit is found by demanding that the multiple charge-exchange flux $d\Gamma_o(E)$ is very small compared to the primary flux of the charge-exchange neutrals due to the incident beam, $d\Gamma_b(E)$. The r-dependence of $d\Gamma_b(r,E)$ is silently omitted and $d\Gamma_b(E)$ is understood as averaged over the beam cross-section n_b. The additional induced flux is found by inserting Δn_o in formula (4) instead of n_b:

$$d\Gamma_o(E) = \int_{-a}^{a} dr \int d^2\rho \, \frac{\Omega_p}{4\pi} \sqrt{4E/\pi} \, dE \, \frac{I_b n_i(r)}{2\pi a^2 e v_i} \langle \sigma_{ex} v \rangle_o \times$$

$$\times \, \varepsilon_{eff}(E) \, \frac{\exp\left\{ - \frac{E}{k_b T(r)} - \int_r^a \frac{dr'}{\lambda(r')} \right\}}{[k_b T(r)]^{3/2}} , \qquad (6)$$

where $d^2\rho$ is the surface of the field of view seen by the analyser. For the transmission, expression (2) is written in terms of the free path length $\lambda(r)$. The flux $d\Gamma_o(E)$ (of charge-exchange neutrals produced by multiple charge exchange) can then be approximated using the mean-value integral theorem:

$$d\Gamma_o(E) = \int d^2\rho \, \frac{\Omega_p}{4\pi} \sqrt{4E/\pi} \, dE \, \frac{I_b n_i(\xi)}{2\pi a^2 e v_i} \langle\sigma_{ex} v\rangle_o \times$$

$$\times \varepsilon_{eff}(E) \, \frac{\exp\{-\frac{E}{k_b T(\xi)} - \int_{\xi}^{a} \frac{dr'}{\lambda(r')}\}}{[k_b T(\xi)]^{3/2}} \, 2a \, , \qquad (7)$$

where $-a < \xi < a$.

Suppose the beam injects at r=0, in a cross-section $r_b \ll a$, this theorem leads in good approximation to:

$$d\Gamma_b(E) = \int d^2\rho \, \frac{\Omega_p}{4\pi} \sqrt{4E/\pi} \, dE \, \frac{I_b A_b}{\pi r_b^2 e v_b} \, n_i(0) \langle\sigma_{ex} v\rangle_b \times$$

$$\times \varepsilon_{eff}(E) \, \frac{\exp\{-\frac{E}{k_b T(0)} - \int_{0}^{a} \frac{dr'}{\lambda(r')}\}}{[k_b T(0)]^{3/2}} \, 2r_b \, . \qquad (8)$$

Now, to minimize multiple charge-exchange effects in the spectrum, its flux, $d\Gamma_o(E)$ should be much smaller than $d\Gamma_b(E)$. This is satisfied by the simultaneous requirements

$$\exp\{-\frac{E}{k_b T(\xi)}\} \, T^{-3/2}(\xi) \leq \exp\{-\frac{E}{k_b T(0)}\} \, T^{-3/2}(0) \, , \qquad (9)$$

$$\frac{n_i(\xi) \langle\sigma_{ex} v\rangle_o}{a v_i} \ll \frac{2A'(\xi) n_i(0) \langle\sigma_{ex} v\rangle_b}{r_b v_b} \, , \qquad (10)$$

where $A'(\xi) = A_b \exp\{-\int_0^a \frac{dr'}{\lambda(r')}\}$.

For ordinary radial temperature profiles in a tokamak, ξ values of 1/2 a to 1/4 a are found.

In all cases, inequality (9) is sufficiently satisfied for energies $E \gtrsim 3/2 \, T(0)$, where T(0) is the ion temperature on axis. This condition is also well-known in passive charge-exchange diagnostics to eliminate profile effects in the temperature determination. In fact we use this inequality for the same reason.

The second inequality (10) is safely satisfied for all energies $E > 3/2\ T(0)$ once it is satisfied for $E = 3/2\ T(0)$. It relates the beam radius and the plasma parameters resulting in a condition for the beam density. In the application in TORTUR, the second inequality is satisfied at least by a factor 5.

e. At high energies, E, special care should be directed to possible complicated contributions to the energy spectrum of particle densities of slowed-down H^+, and protons from dissociated H_2^+ and H_3^+ beam species at 1/2 and 1/3 of the injection energy respectively. As is well-known, the ion source produces non-negligible amounts of H_2^+ and H_3^+, without mass separation. A measure for the value of E above which the perturbation due to alien trapped particles plays a significant role, is obtained by requiring that

$$\int_E^\infty \frac{\Delta n}{\Delta E}\, dE \geq \bar{n}\ (b)\ , \tag{11}$$

where $\bar{n}(b)$ is the upper bound of trapped particles:

$$\bar{n}(b) = \frac{I_b \tau_{sld}(E)}{e.vol}\ (1-A_b)\ . \tag{12}$$

τ_{sld} (slowing down) is the time for beam particles to relax to an energy E; vol is the volume occupied by trapped particles, which is close to the torus volume. $\Delta n/\Delta E$ is given by expression (1).
Inserting the relevant values of TORTUR and the probing beam, this leads to

$$E_{max} \leq (5\text{-}6) \times T(0)\ ,$$

where T(0) is the central ion temperature.

2. DIAGNOSTIC SET-UP FOR THE DETERMINATION OF THE ION ENERGY DISTRIBUTION

2.1 The experimental arrangement

The experimental arrangement used in the TORTUR tokamak is shown schematically in Fig. 2.

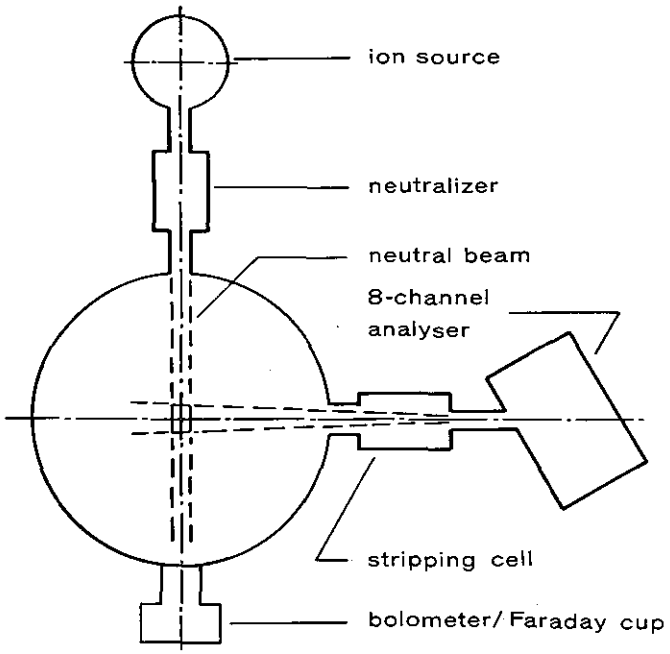

Fig. 2. The experimental arrangement for an active diagnostic based on enhanced charge-exchange processes.

The ion source is a so-called duopigatron source. Its functioning is extensively described by Bonnal et al. [4]. In Fig. 3 the electric circuit of the extraction system for the ion source and the bolometer/Faraday cup is shown schematically. The scheme is discussed in detail by Brocken [5] and Van Dijk [6].

The extraction voltage of the ion source lies between 20-30 kV. The current extracted from the source is maximally about 4 A. A neutral current (I_b) of about 1 ampere equivalent can be attained at the focus [6]. Losses are caused by losses in the beam transmission line and by inefficiency of the neutralizer [7]. The neutral beam injects vertically. The angle of the divergence cone of the neutral beam is $2.45 \pm 0.15^{\circ}$.

The neutral beam diagnostics, a bolometer/Faraday-cup combination, are positioned on the opposite side of the torus (Fig. 3). These diagnostics as well as the beam line (from source to torus) were described by Brocken [5].

When the toroidal magnetic field is present the neutral beam current densities measured with the Faraday cup are in the range of 10-20 mA/cm^2. Figure 4 shows a typical Faraday-cup signal. During 5 ms, the operation time of the source, the neutral current density drops from 15 mA/cm^2 to 10 mA/cm^2.

The bolometer can also be used to measure the beam intensity. The thermocouples of the calorimeter are followed by 400× amplifiers. The calibration of the bolometer output signal is then given by $\Delta V = 6.8\times10^{-2}\ E_b I_b \Delta t$, where ΔV is the output signal voltage of the amplifier in V, E_b the beam current density in mA/cm^2. The extraction time Δt is expressed in seconds. The time response of the bolometer is about 0.3 second. In the experimental period discussed, the bolometer was used, in particular, to adjust the ion source in a vertical position. Figure 5 shows an example of the measured bolometer signal.

The following provisions and changes have proved to give remarkable improvement in the performance of the probing beam:

- The 'stop-circuit' that serves to stop the extraction, was removed to eliminate the disturbance caused by the pulse of this circuit.
- The resistance between the starting circuit and the third grid - the decelerator grid - turned out to be 950 Ω for optimal performance as far as the extraction was concerned.
- Effective - separate - earthing of various parts has given considerable improvement in the performance.

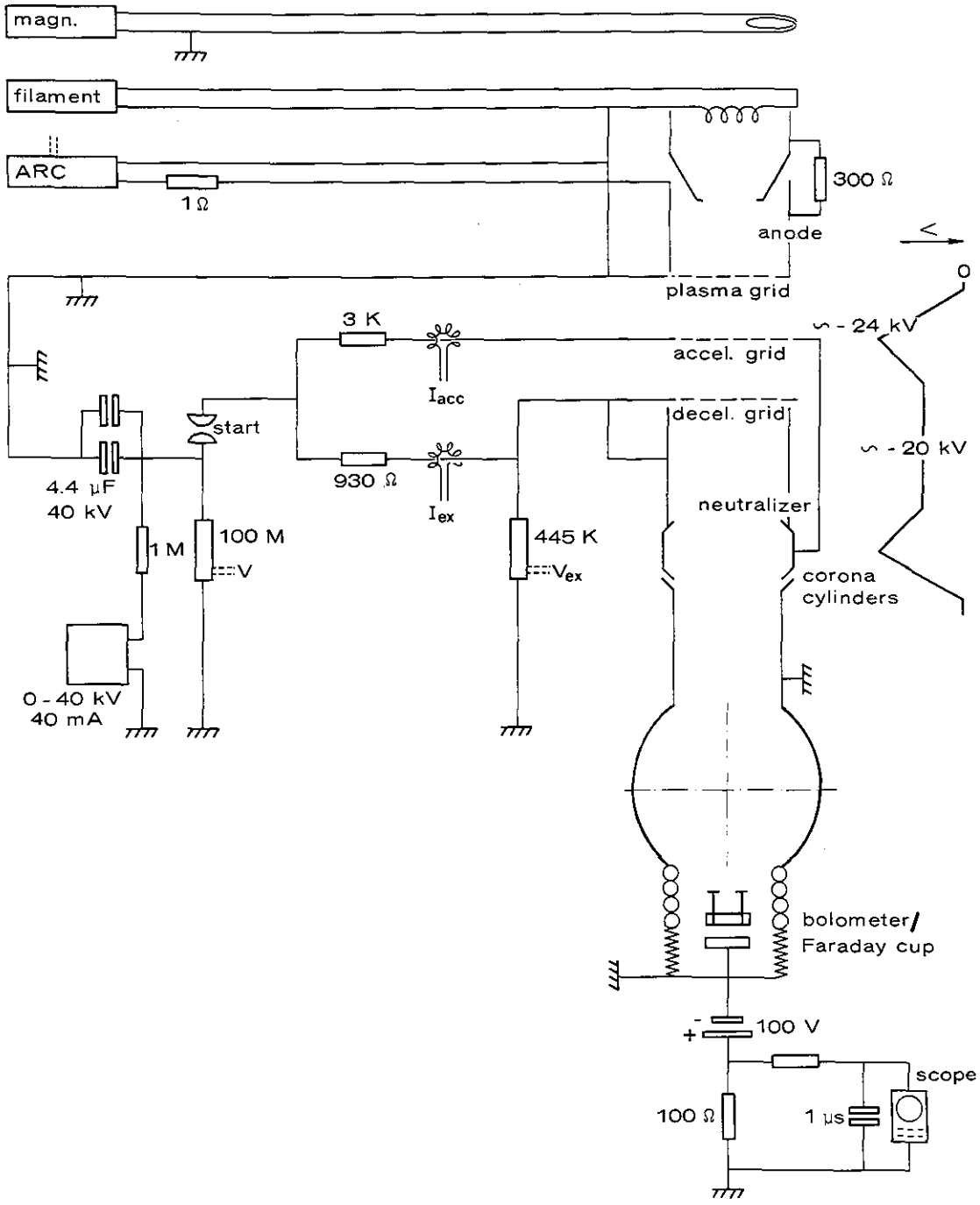

Fig. 3. Scheme of the electrical circuit, the extraction system and the beam diagnostics.

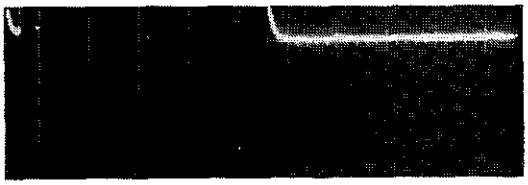

→ t (ms/div.)

Fig. 4.
An example of the Faraday-cup signal to measure the neutral density (5 mA/div).

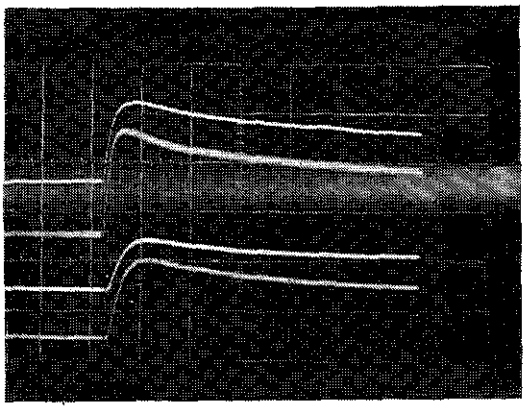

→ t (ms/div.)

Fig. 5.
An example of the bolometer signal indicating the vertical position of the source.

2.1.1 The arc discharge

Requirements for sufficient ionization of neutral hydrogen were described by Van Dijk [6], Huizenga [8], and Green [9].

The optimal value of the arc voltage is some 200 V. Below 100 V, it is not possible to start an arc current.

In the tungsten filament a current of 65-70 A is mostly used. More than 75 A is not allowed and below 60 A it is not possible to start a discharge.

The influence of the magnetic field is most important. In Figs. 6a-f the dependence of the magnetic field on the arc current can be seen clearly. Moreover, these figures show that a magnetic field of less than 350 gauss cannot possibly produce a stable arc current. 500 gauss proved to be a correct adjustment. The arc current depends strongly on the hydrogen gas inlet and it was found that during one day of experimenting the gas inlet had to be increased to obtain the same current. A start value of 2.5 torr l/s was normally used.

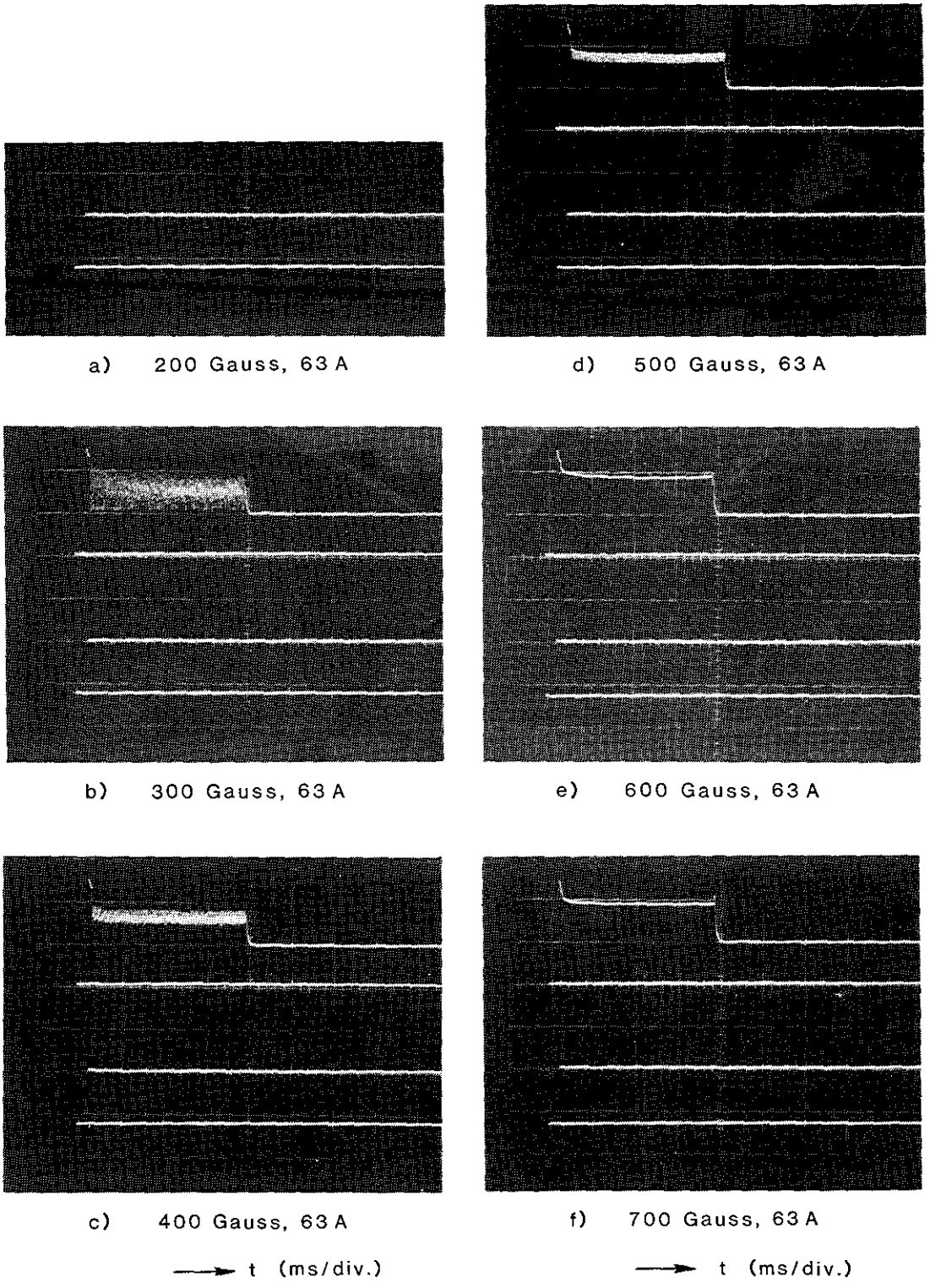

Figs. 6a-f. Arc currents showing the influence of the applied magnetic fields.

2.1.2 The triggering

The trigger signals are transmitted via light conductors and, with adjustable delay times, various trigger times are obtained. For the principal operating parameters triggering instances, duration and values are shown in Fig. 7.

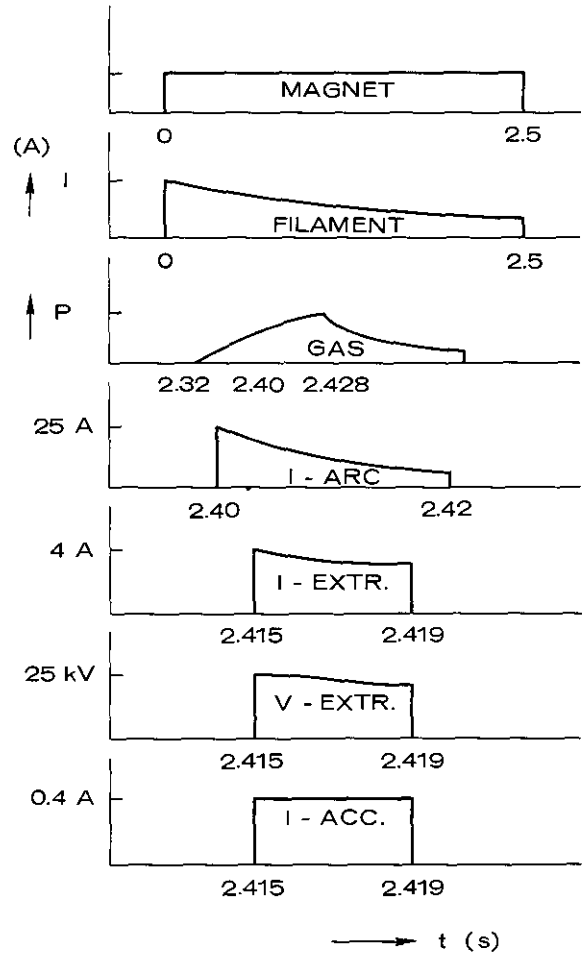

Fig. 7. Time scheme of the source triggering.

2.1.3 The conditioning

It took several days of conditioning before a reasonable extraction was achieved. This can be seen in Fig. 8 at the microscopic break-downs on the various signals.

Figure 9 shows the signals after the conditioning of the ion source. (The increase of the arc current is due to an extra gas inlet caused by triggering of the start pulse.)

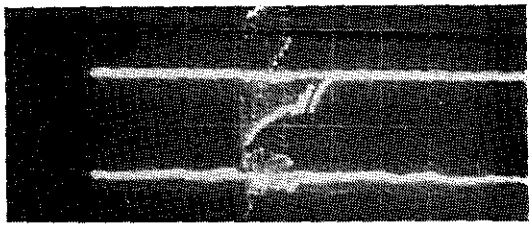

Fig. 8.
Microscopic break-downs in the extraction during conditioning.
a. Arc current 20 A/div.
b. Extraction current 4.7 A/div.
c. Extraction voltage 10.7 kV/div.
d. Acceleration current 0.6 A/div.

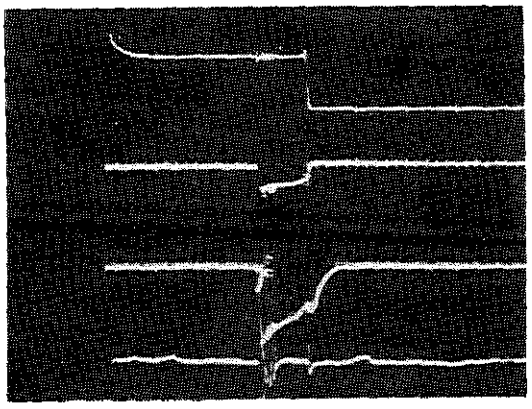

Fig. 9.
Signals after the source is conditioned.
a. Arc current 20 A/div.
b. Extraction current 4.7 A/div.
c. Extraction voltage 10.7 kV/div.
d. Acceleration current 0.6 A/div.

2.2 The analysing system

The method used to determine the energy distribution of the neutral particle flux is to ionize the neutral particles in a helium gas cell and, subsequently, record the fluxes in the 10 channels of an electrostatic energy analyser.

2.2.1 The helium cell

After having left the plasma, the neutrals pass a stripping gas cell of 10 cm length. Helium is used as a stripping gas because even at relatively low energies the ionization cross-section of H + He collisions is well-known [10].

The helium pressure is usually 1 mtorr. Other helium pressures up to 5 mtorr showed hardly any difference in the number of detected particles.

2.2.2 The electrostatic energy analyser

Behind the stripping cell, the ion flux is collimated and enters the energy analyser. A homogeneous electrostatic field causes an energy selection of the ions in a spatial direction perpendicular to the applied field. The ions are transmitted through a highly transparent grid and post-accelerated over 25 kV towards a secondary emission plate. The secondary electrons produced have an energy independent of the original ion energy. The electrons leave the emission plate almost perpendicularly and pass various grids before they are detected in one of the 10 channels as a function of position. A channel consists of a phosphor coupled to a photomultiplier by a light-guide. The position of detection x, i.e. the location of the photomultiplier, is then directly related to the energy E of the neutral particles by $E \approx 1/2 \times eF$, where e is the elementary charge and F represents the analysing field strength.

The energy resolution is given by

$$\frac{\Delta E}{E} = \frac{\Delta x_1 + \Delta x_2}{x} ,$$

where Δx_1 and Δx_2 represent the width of the entrance slit and of the slit in front of the phosphor.

$\Delta E/E$ varies from 0.6% to 12%, corresponding with the farthest and the nearest location of the photomultiplier, respectively.

The positions of the detectors in the analysing system are given in Table I.

TABLE I

channel	x (mm)
1	46
2	-
3	114.5
4	148.5
5	182.0
6	216.0
7	250.8
8	284.0
9	317.2
10	352.0

(Channel 2 is a dummy.)

2.2.3 The calibration of the photomultipliers

Prior to measuring the energy distributions, the arrangement was calibrated. With a pulse-height analyser, a pulse-height distribution was composed and two calibration coefficients could be deduced for each photomultiplier [11].

The results of a least square fit with parameters λ and μ of the measured curve with the theoretical pulse-height distribution,

$$\frac{dN}{dh} = K \frac{\exp(-h/\mu)}{\sqrt{\lambda h/\mu}} I(2\sqrt{\lambda h/\mu}) \quad , \qquad (13)$$

are shown in Table II.

Here, dh is the pulse-height increment at the terminating capacitor of the photomultiplier, caused by one electron that reaches the first dynode;

μ, a proportionality constant, represents the average pulse-height enhancement caused by one electron that reaches the first dynode;

λ is the average number of electrons arriving at the first dynode of the photomultiplier per incident ion;

I is the modified Bessel function of the first kind and first order, and

K is a normalization constant.

The pulse-height interval dh should be chosen so short that the probability that the pulse-height increment is caused by two or more electrons may be neglected.

TABLE II.

Calibration coefficients of the photomultipliers of the energy analyser during the period March 1982 till September 1982

photomultiplier no.	λ	μ (in V)
1	3.740	2.535
2	1.000	0.000
3	4.646	2.942
4	4.016	2.066
5	5.741	3.822
6	8.247	6.089
7	7.796	5.757
8	2.430	1.395
9	2.304	1.340
10	2.569	2.511

2.2.4 The evaluation of the spectrum from the analysed fluxes

The measured energy distribution is not entirely local, but it is an integral value over the finite width (3 cm) of the neutral beam. Figure 10 shows the signals of the particle analyser during one discharge.

An energy distribution comprising the complete energy range up to 5 keV is composed of 4 to 6 settings of the electrostatic analyser. For example: 456 V, 758 V, 1277 V, 2133 V, 2800 V. The energy of the particles in a channel is determined by: $E_p = 0.2 \times n \times V_{an}$, where n is the channel's number (1-10), V_{an} is the setting of the electrostatic analyser, and E_p is the energy of the particle in eV. The signals are corrected for the background and disturbing signals: a measurement without injection with the neutral beam is subtracted from a measurement with an injection. This correction is not entirely effective for the lower energies. Injection inevitably raises the flux of low-energy neutrals due to emission from the walls, caused by collisions of the injected neutrals against the wall.

This low-energetic neutral flux is also raised by the trapped beam particles in the outer part of the torus. These are the main reasons that after correction for the background (correction for the trapped beam particles has not been done due to the unknown width of this distribution in the time) the measured flux remains higher than the expected value.

Four discharges with the same analysing voltage, three with an injecting probe and one discharge without a beam, are handled in the same way as described. The calibration factors used for these measurements are shown in Table II. The data of these three discharges are averaged and give, in principle, nine points in the resulting energy spectrum for some time interval (one channel is a dummy).

This procedure is repeated for four to six settings of the analysing voltage to give the ultimate energy distribution of the neutrals, i.e. a spectrum of the measured flux is the energy of the neutrals (see Fig. 11). This yields 20 to 40 points in the entire energy range. By varying the injection time, the energy distribution of the ions in the centre can be measured at different times. The time dependence of the central ion temperature can be obtained by attaching temperatures to the energy distributions.

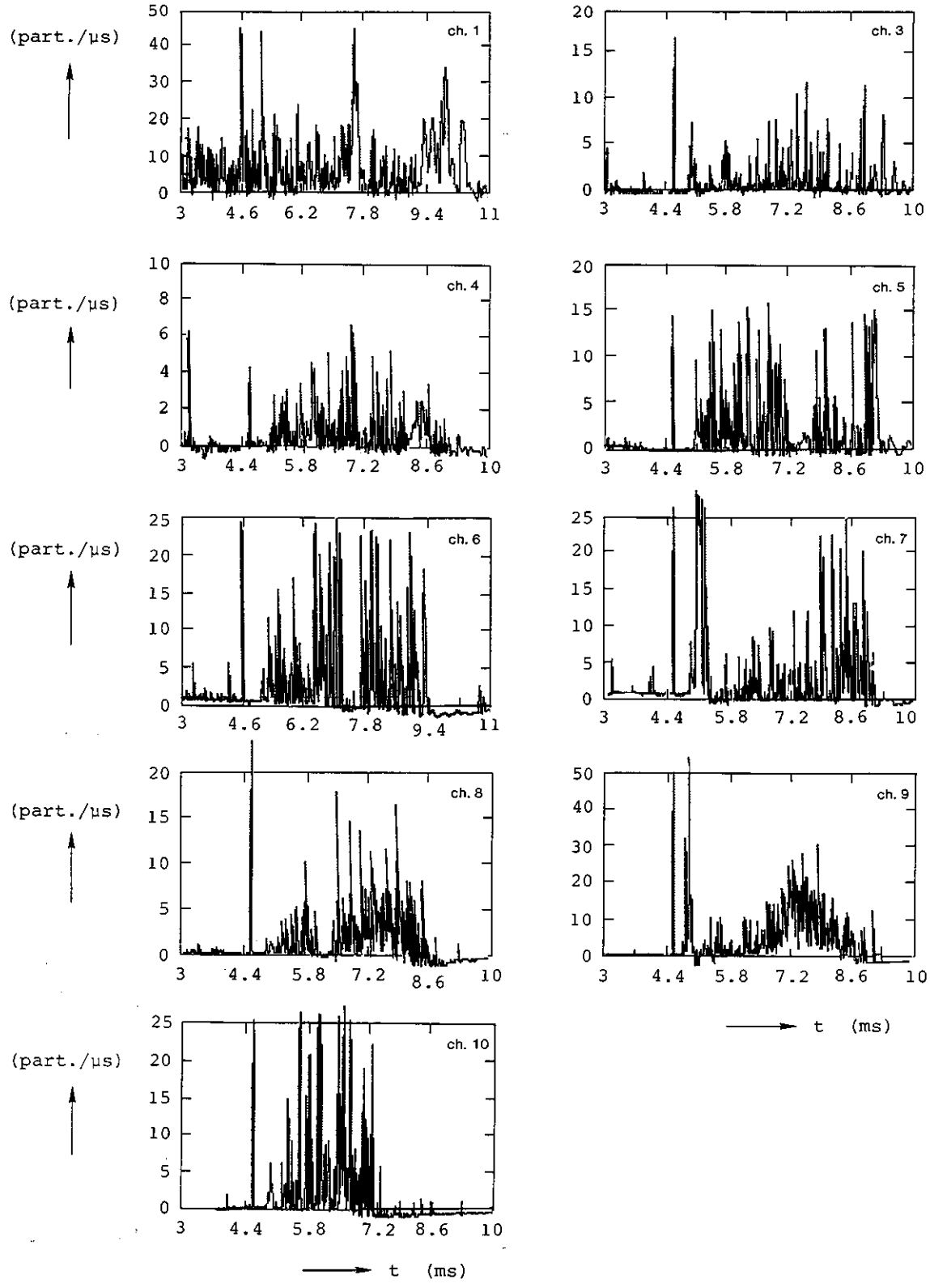

Fig. 10. Signals of the electrostatic analyser during one discharge. Beam injection starts at t = 4.6 ms and lasts 5 ms. I_{beam} = 150 mA; B_0 = 3.2 T; n_{pl} = 5.0×10^{19} m^{-3}. The time resolution is 12.8 μs.

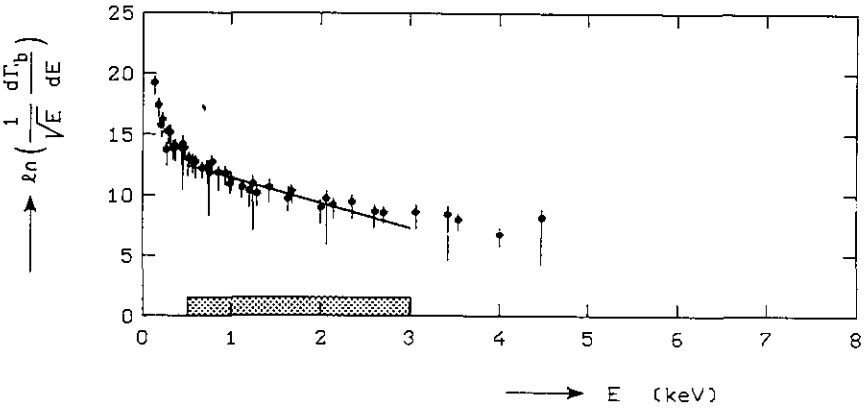

Fig. 11. The energy spectrum measured with neutral injection at r = 5×10^{-3} m, at t = 8.5 ms. A temperature of 495 eV can be deduced from the slope of a line in the energy range 500 eV up to 3000 eV.
The discharge conditions were: B_0 = 3.2 T, n = 6×10^{19} m^{-3}.

To this end an energy interval has to be selected. This is done with due regard to the lower and upper limits of the energy interval in 1.2 (Eqs. (9), (10) and (11)). A negative least square fit gives the central ion temperature provided that the absolute magnitude of the extrapolated straight line part to zero energy represents the bulk of the plasma. The calculated logarithmic flux as a function of the ion temperatures for various densities with lim E → 0 can be found as follows.

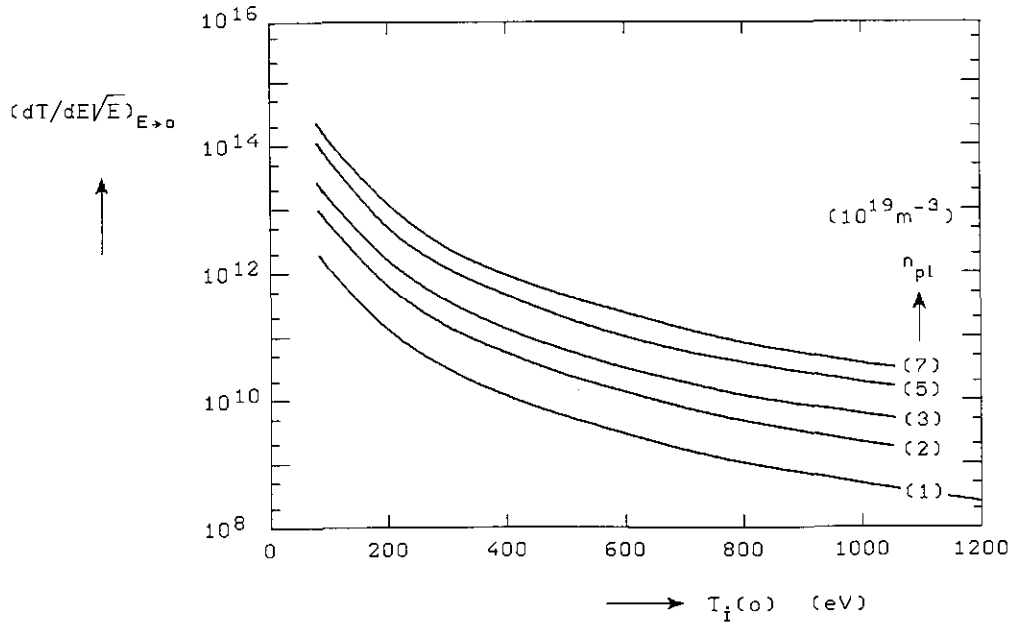

Fig. 12. Theoretical flux of the particles emerging from the plasma as a function of the temperature for different densities.

Formula (4) of Chapter 1 reads for r=0 as:

$$d\Gamma_b = \sqrt{4/\pi}\,\frac{\Omega_p}{4\pi}\,A_b(0,E)\,A_c(0,E)\,n_b n_{pl}(0)\,\langle\sigma_{ex}v_b\rangle\,\left(\frac{E}{k_B T(0)}\right)^{3/2} \times$$

$$\times \exp\left[-\frac{E}{k_B T(0)}\right]\,\frac{\Delta E}{E}\,dV_{br} \ .$$

Division of both sides of this equation by $\sqrt{E}\,\Delta E$ and taking the limit $E \to 0$ leads to:

$$\ln\frac{d\Gamma_b}{\sqrt{E}\,dE} = \ln c + \ln n_{pl} - \frac{3}{2}\ln T_i \ . \qquad (14)$$

n_{pl} is the plasma density $[m^{-3}]$ and T_i is the plasma ion temperature $[eV]$.

$$c = \sqrt{4/\pi}\,\frac{\Omega_p}{4\pi}\,A_b(0,E)\,A_c(0,E)\,n_b\langle\sigma_{ex}v\rangle_b\,dV_{bp} \ .$$

Inserting typical TORTUR injection data for r=0:

Ω = 1.15×10^{-5} sterad ,
A_b = 0.75
A_c = 0.25 [Ref. 5].
n_b = 4.69×10^{14} m^{-3} (j = 150 A/m^2, V = 20 kV)
$\langle\sigma_{ex}v\rangle_b$ ≈ 8.0×10^{-14} $m^3\ s^{-1}$
dV_{bp} = 1.0×10^{-5} m^3 ,

gives $\ln c = -24.73$.

In view of possible wall effects which generally increase the flux, this value of $\ln c$ should be considered as a minimum: if the measured neutral flux is less than the predicted flux, the data should be mistrusted. In Fig. 12 the result of the calculation is shown for various plasma densities in TORTUR.

Now we will discuss the general nature of a beam enhanced neutral flux analysis, by examining Fig. 11.

The spectrum may be divided into three regions:

A. A low-energetic region with $E \leq 3/2\ T_i$. (T_i is the central ion temperature.) This low-energetic region originates from particles from outer regions of the plasma and has a relatively high flux. If a temperature is to be attached to this region, these temperatures are in the order of 50-100 eV.

B. An intermediate region representing energies from charge-exchange neutrals from the centre of the plasma due to the probing beam. Energies of this region are between $E \approx 3/2\ T_i$ and $E \approx 5$ to $6\ T_i$.

C. A part of the spectrum that contains energies larger than 5 to 6 T_i. This part comprises the non-maxwellian "tail" of the energy distribution which might also contain thermalized dissociation products of H_2^+ and H_3^+ ions of the injected beam [12].

3. RESULTS OF MEASUREMENTS FROM BEAM ASSISTED CHARGE EXCHANGE

In the following figures the ion temperature at the axis is shown as a function of time. Only during part of the discharge (4-5 ms) the beam is present. In the figures the time the beam injects is indicated on the abscis. At other times we had therefore to rely on the passive method of analysis to determine the ion temperature. In that case the ion temperatures are obtained from the asymptotic slope for higher energies because only the higher energy part of the flux is predominantly composed of charge-exchange ions from the central plasma regions. The electron temperatures and the plasma current which belong to the chosen examples of ion temperature measurements are also shown.

Before showing examples of the time evolution of the ion temperature for various discharge conditions, the electron temperature and the plasma current are shown in Figs. 13 and 14 as a function of time. In Figs. 15 and 16, respectively, the almost linear increase of T_e and n_e with the plasma current in TORTUR III are shown.

Now a series of measurements of the ion temperature are given in the Figs. 17-19. In the captions comments about various discharge conditions are given.

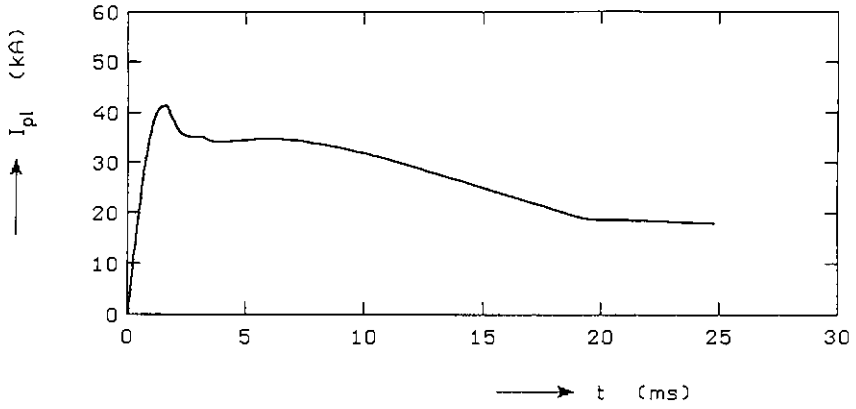

Fig. 13. A typical example of the plasma current.

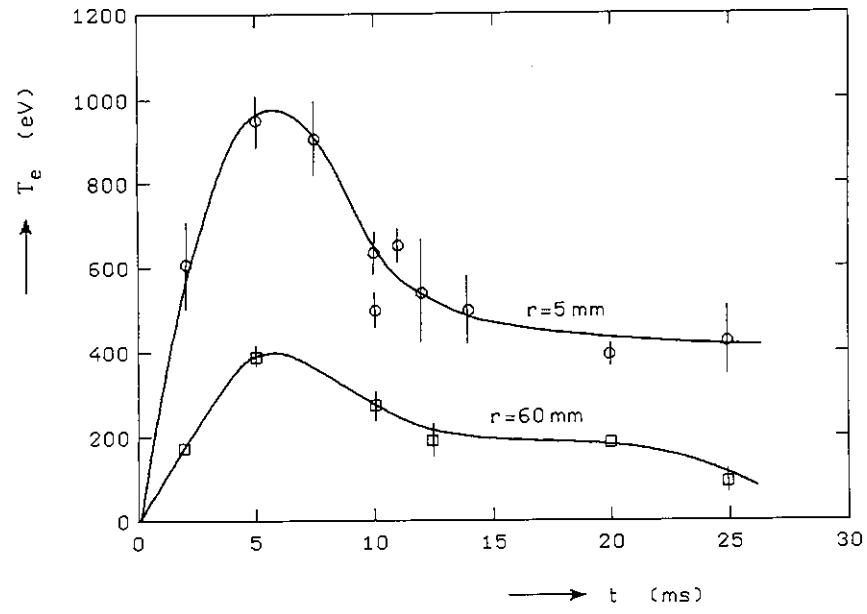

Fig. 14. The electron temperatures which belong to currents as shown in Fig. 13.

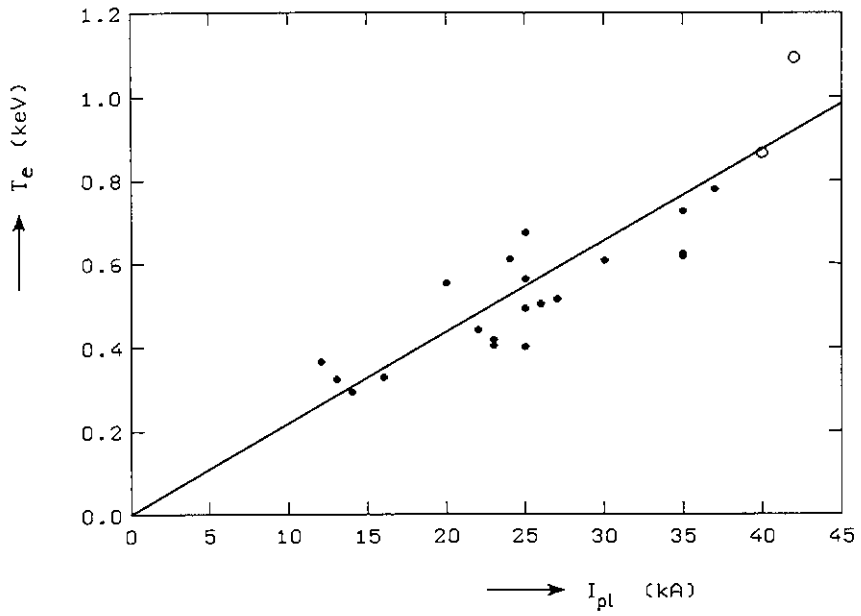

Fig. 15. The electron temperature as a function of the plasma current in the TORTUR III tokamak. B_o = 2.9 T.

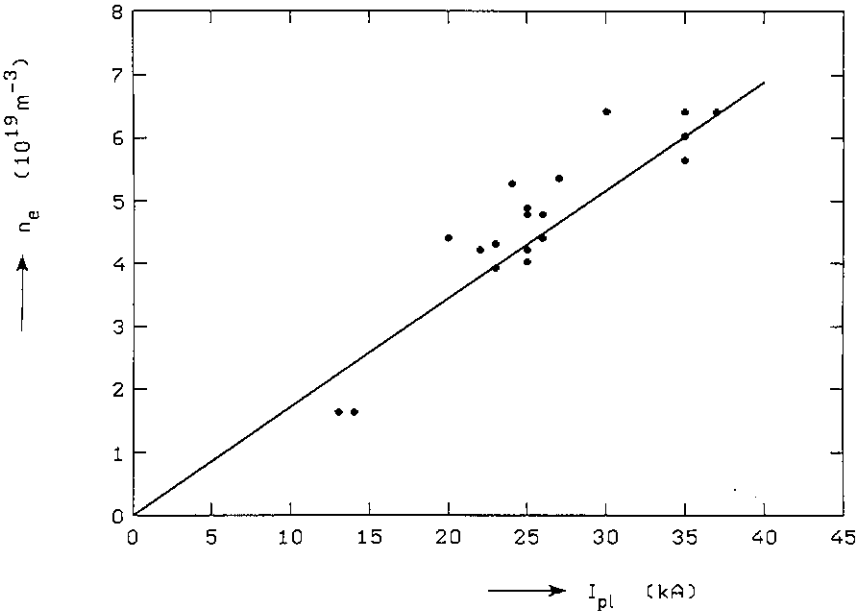

Fig. 16. The plasma density as a function of I_{pl}. B_o = 2.9 T.

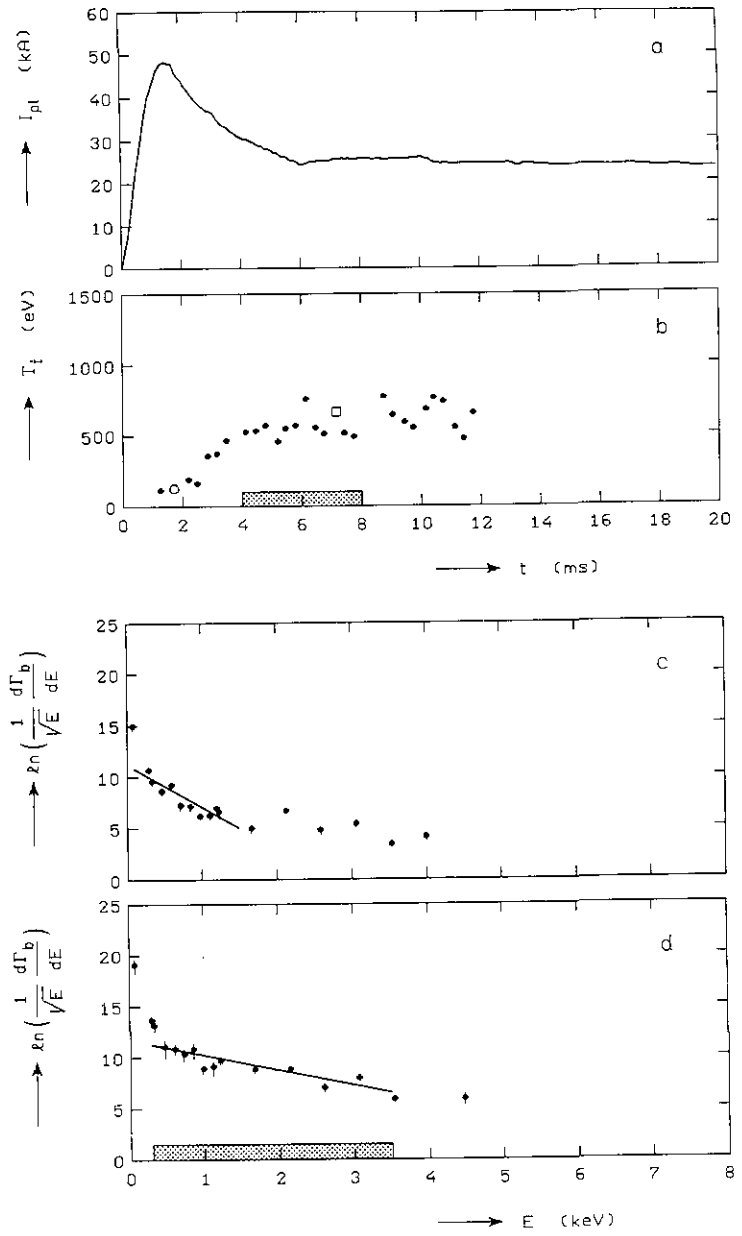

Fig. 17.

Ion temperatures as a function of time.
Discharge conditions are: B_o = 2.9 T: $n_e = 4.1\times10^{19}$ m^{-3}:
$T_e(0)$ = 630 eV in the plateau.
a. I_{pl} vs time: b: time evolution of T_i during early times of the discharge. The active period of determination (injection of beam 4-8 ms) is indicated by the bar on the abscis. The ion temperatures - final value about 650 eV at t = 6 ms - show relatively large fluctuations both in the active and passive period of determination probably due to strong density fluctuations from low frequency turbulence in the outer layers of the plasma [13], [14]: examples of energy distributions which belong to an early determination (passive: the open circle) and during beam injection (active: the open square) are shown in c and d, respectively. The bar in Fig. 17d indicates the prescribed energy interval for the temperature determination. Integration time for each point: 100 microseconds.

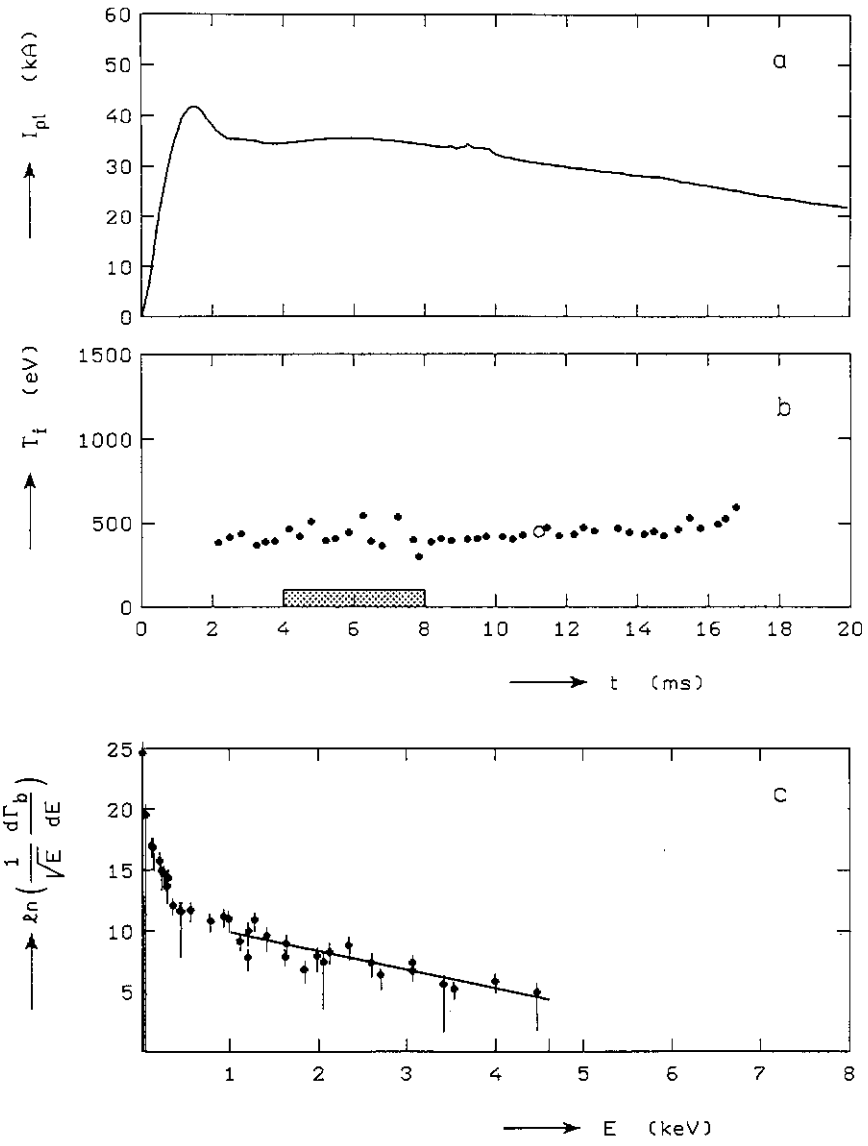

Fig. 18.

T_i vs time. Discharge paramaters: B_0 = 2.9 T; n_e = 5.6×10^{19} m^{-3};
$T_e(0)$ = 730 eV in the plateau.
a: I_{pl} vs t: b: T_i vs t during injection (bar on abscis: active)
(without: passive). It is often noticed that during the injection period the plasma exhibits stronger fluctuations in T_i than without injection. The presence of the beam might have triggered low-frequency drift waves: c: an example of an energy distribution in the passive phase (see open circle in Fig. 18b).

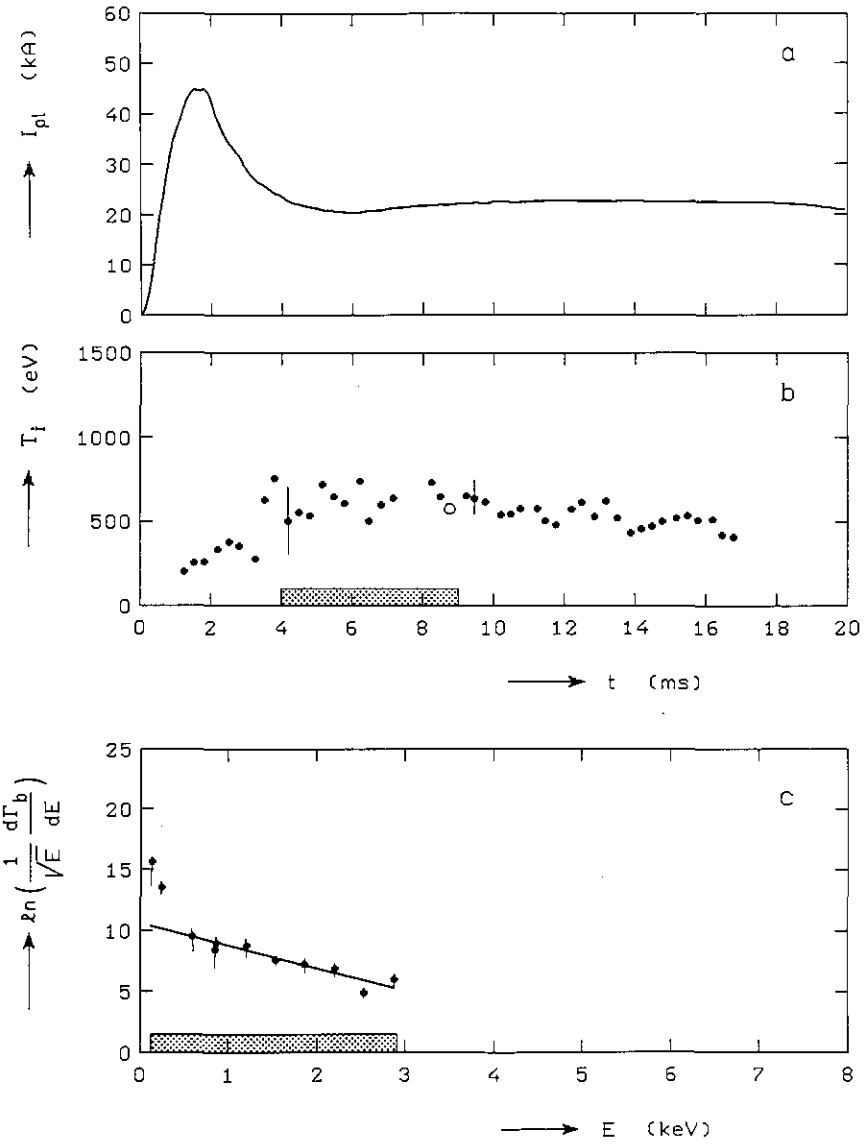

Fig. 19.

T_i vs t at a lower toroidal field strength: B_0 = 1.8 T. Other discharge parameters: $n_e = 4.3\times10^{19}$ m^{-3}: plateau value $T_e(0)$ = 450 eV. a: I_{pl} vs t; b: T_i vs t. The ion temperatures (650 eV) are always higher than T_e. The errors in the determination are typically as shown by the bars; c: a specimen determination of T_i during the active phase (open circle in Fig. 19b). The bar on the abscissa indicates the energy region valid for the determination.

4. CONCLUSIONS

It has been demonstrated that the use of a 20-30 keV hydrogen atom probing beam leads to a strong increase of the local charge-exchange processes above the natural background, thus enabling local and time-resolved measurements of the ion temperature.

It turns out that variation of the beam does not change the charge-exchange flux very much in the range between 20 and 30 keV. This is because an increase in the beam transmission, due to a higher beam energy, is compensated by a decrease in the cross-section for charge exchange. At first sight, the highest beam current densities should be chosen. However, though trivial, care has to be taken to avoid appreciable plasma heating. For injection times in TORTUR of about 5 ms at 25 kV and a trapping efficiency of about 50%, the heating amounts up to 65 eV per A equivalent. Heating effects of the predicted magnitude have indeed been observed.

The measurements have to be corrected for the presence of charge-exchange neutrals emerging from the plasma itself (the "background"). It is difficult to make a precise estimate of the magnitude of this contribution. Calculation of the production of neutrals arising from radiative recombination, performed by Dnestrovskij [2] and by our group [3], show this effect to be small at densities below 10^{20} m^{-3}. Of course, the experiment itself helps to judge the contribution of the background.

For injection near the centre, the flux increase above the background amounts to 5-10 times, as can be seen in Fig. 10. Clearly, this method cannot be applied in large cross-section tokamaks because beam losses become too large and multiple charge exchange (thus re-ionization) of charge-exchange neutrals starts to play an ever-increasing role.

A correction for the background flux can be obtained by subtraction. This is an effective procedure at least in the range of higher energies.

For lower energy, a complete compensation is not possible because the injection with the beam increases the neutral density at the periphery due to degassing of energetic ions hitting the vessel wall.

The energy spectrum is perturbed by an increase of the background neutral density due to charge exchange of plasma ions by the injected beam atoms. Profile effects have to be eliminated, which gives a condition that $E \geq 3/2\ T_i(0)$. This condition is in fact the same for eliminating profile effects in passive charge-exchange diagnostics. The energy spectrum is also perturbed by the possible contribution of trapped and slowed-down H^+, H_2^+ and H_3^+ species of the beam. Without mass separation, hydrogen ion sources can produce copious fractions of H_2^+ and H_3^+ at reduced beam energies (i.e. 1/2 and 1/3, respectively). For TORTUR it can be shown that $E < (5\text{-}6)T_i(0)$. The presence of H_3^+ and slowed-down H_2^+ and H^+ for $E > (5\text{-}6)T_i(0)$ is clearly visible in Fig. 11. The spectrum of partially thermalized trapped beam particles shows a complicated asymptotic behaviour at low energies. In TFR, detailed measurements of slowed-down spectra due to heating beams show similar features [15].

The active charge-exchange method will fail when multiple charge exchanges occur at a high rate between the beam region and the plasma edge, i.e. when $na\sigma_{ex} \gg 1$. This results in an upper limit for the density of $(6\text{-}7)\times 10^{19}$ m^{-3}, with a beam energy of 25 keV for TORTUR when applying this method.

Satisfactory agreement is found between central ion temperatures determined with the active method (beam probe) and from the estimates using the asymptotic slopes of the energy distributions.

ACKNOWLEDGEMENTS

The authors are very grateful to Prof.Dr. H. de Kluiver for his critical discussion of the manuscript. They express their gratitude to Dr.Ir. H.W. Piekaar, H.W. van der Ven, B. de Groot, C.J. Barth and H.J. van der Meiden. The efforts of the technical departments of the Institute are highly appreciated.

This work was performed as part of the research programme of the association agreement of Euratom and the "Stichting voor Fundamenteel Onderzoek der Materie" (FOM) with financial support from the "Nederlandse Organisatie voor Zuiver-Wetenschappelijk Onderzoek" (ZWO) and Euratom.

REFERENCES

[1] Rehker, S. and Speth, E., IPP 2/217, Max-Planck-Institut für Plasmaphysik, Garching (1974).
[2] Dnestrovskij, Yu.N., Lysenko, S.E. and Kislyakov, A.I., Nucl. Fusion 19 (1979) 293.
[3] Brocken, H.J.B.M. and Kluiver, H. de, Plasma Phys. 25, (1983) 317.
[4] Bonnal, J.F., Druaux, J. and Oberson, R., Eur-CEA-FC-791, Fontenay-aux-Roses (1975).
[5] Brocken, H.J.B.M., Rijnhuizen Report 81-137 (1981).
[6] Dijk, J.A.W. van, Internal Report I.R. 79/010, Nieuwegein (1979).
[7] Green, T.S., Rep. Prog. Phys. 37 (1974) 1257.
[8] Huizenga, W., Rijnhuizen Report 63-11 (1963).
[9] Green, T.S. and Goble, C., CLM-P-352 and CLM-P-353, Culham Laboratory, Abingdon (1973).
[10] Adlam, J.H. and Aldcroft, D.A., RLM-R-100, Culham Laboratory, Abingdon (1969).
[11] Brocken, H.J.B.M., Rijnhuizen Report 80-122 (1980).
[12] Brocken, H.J.B.M., Kluiver, H. de, Hendriks, F.B., Plasma Phys. 26 (1984) 749.
[13] Kluiver, H. de, et al., Phys. Lett. 94A (1983) 156.
[14] Huussen, F., Ikezawa, S., Kluiver, H. de, Plasma Phys. 27 (1985) 4.
[15] IFR Group, Nucl. Fusion 23 (1983) 4.

[16] Belyaev, V.A. et al., Sov. Phys. JETP, Vol. 25.5 (1967) 777.
[17] Fite, V.A. et al., Phys. Rev. 112 (1958) 1161.
[18] Fite, V.A., Phys. Rev. 119 (1960) 663.
[19] McClure, G.W., Phys. Rev. 148 (1966) 47.
[20] Gilbody, H.B. et al., Proc. Roy. Soc. 227A (1964) 137.
[21] TORTUR Team - Kluiver, H. de, et al., Proc. 10th Int. Conf. on Plasma Phys. and Contr. Nucl. Fusion Res., London, September (1984) Vol. 1, p. 375.
[22] TORTUR Team - Kluiver, H. de, et al., Proc. 12th Eur Conf. on Contr. Fusion and Plasma Phys., Budapest, September (1985) Vol.II, p. 272.
[23] Lopes Cardozo, N.J., "Anomalous plasma heating induced by modulation of the current-density profile", Thesis University of Utrecht 1985, Rijnhuizen Report 85-160 (1985).